

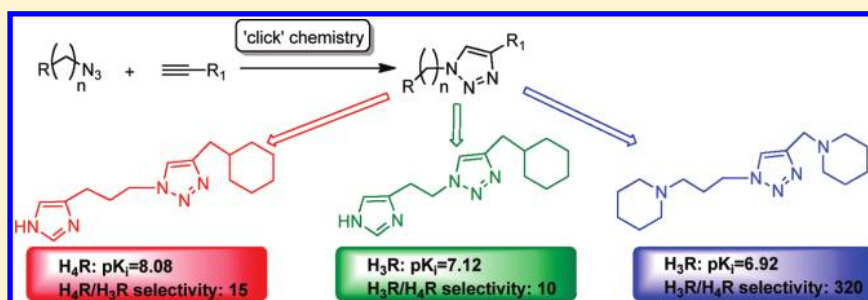
Triazole Ligands Reveal Distinct Molecular Features That Induce Histamine H₄ Receptor Affinity and Subtly Govern H₄/H₃ Subtype Selectivity

Maikel Wijtmans,* Chris de Graaf, Gerdien de Kloe, Enade P. Istyastono, Judith Smit, Herman Lim, Ratchanok Boonnak, Saskia Nijmeijer, Rogier A. Smits, Aldo Jongejan, Obbe Zuiderveld, Iwan J. P. de Esch, and Rob Leurs

Leiden/Amsterdam Center for Drug Research, Division of Medicinal Chemistry, Faculty of Exact Sciences, VU University Amsterdam, De Boelelaan 1083, 1081 HV Amsterdam, The Netherlands

S Supporting Information

ABSTRACT:



The histamine H₃ (H₃R) and H₄ (H₄R) receptors attract considerable interest from the medicinal chemistry community. Given their relatively high homology yet widely differing therapeutic promises, ligand selectivity for the two receptors is crucial. We interrogated H₄R/H₃R selectivities using ligands with a [1,2,3]triazole core. Cu(I)-assisted “click chemistry” was used to assemble diverse [1,2,3]triazole compounds (6a–w and 7a–f), many containing a peripheral imidazole group. The imidazole ring posed some problems in the click chemistry putatively due to Cu(II) coordination, but Boc protection of the imidazole and removal of oxygen from the reaction mixture provided effective strategies. Pharmacological studies revealed two monosubstituted imidazoles (6h,p) with <10 nM H₄R affinities and >10-fold H₄R/H₃R selectivity. Both compounds possess a cycloalkylmethyl group and appear to target a lipophilic pocket in H₄R with high steric precision. The use of the [1,2,3]triazole scaffold is further demonstrated by the notion that simple changes in spacer length or peripheral groups can reverse the selectivity toward H₃R. Computational evidence is provided to account for two key selectivity switches and to pinpoint a lipophilic pocket as an important handle for H₄R over H₃R selectivity.

INTRODUCTION

The neurotransmitter histamine exerts its biological action through four histamine receptors, which all belong to the superfamily of G protein-coupled receptors (GPCRs).¹ Whereas the histamine H₁ and H₂ receptors are proven targets for blockbuster drugs, the H₃R and H₄R both bear promise to reach that stage in the near future. The H₃R was discovered in 1983² and cloned in 1999.³ Ever since, intensive research has taken place to discover H₃R ligands. Consequently, the past decade has seen the emergence of many different classes of H₃R antagonists.^{4–7} The newest addition to the histamine receptor family is the H₄R. Since its discovery in 2000, it has attracted much interest from academia and industry alike.^{8,9} The H₄R is widely expressed on hematopoietic and immune cells, where it mediates chemotaxis of eosinophils and mast cells.^{10,11} Therefore, it is believed to play an important role in inflammation and immune responses with possible applications in diseases such as inflammatory bowel

disease, allergic asthma, and pruritis.^{9,12} More recently, possible roles in pain modulation and (breast) cancer have been revealed.^{13,14} The high interest of medicinal chemists for H₄R has manifested itself in an increasing development of small molecules able to modulate H₄R. A few selective small-molecule agonists have been disclosed^{15–17} and are useful tools in H₄R research.^{18,19} From a therapeutic point of view though, most of the focus has been on H₄R antagonists, and several different classes of H₄R antagonists have been disclosed to date.^{14,20–23} H₄R antagonists have proven very useful in the confirmation of postulated roles of the H₄R.^{14,21,24–26}

A reoccurring issue in the development of small H₄R ligands is the selectivity between H₄R and H₃R. These two receptors share the highest homology within the histamine receptor family (31% overall, 54% in the transmembrane region).⁸ This implies that

Received: October 18, 2010

Published: February 24, 2011

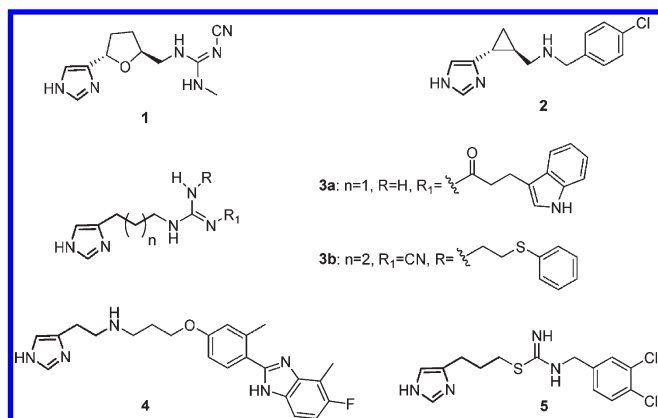


Figure 1. Exemplary imidazole-containing H_4R ligands with selectivity over H_3R .

potential selectivity issues are to be expected. Indeed, several classical H_3R tool compounds, such as thioperamide and clobenpropit, also display considerable H_4R affinities.¹⁶

In the area of non-imidazole ligands, H_4R selectivities have been proven to be readily accessible.²⁴ A fundamentally interesting and intrinsically challenging task is to achieve selectivity with imidazole-containing ligands, as both receptors are equipped with imidazole-binding pockets. H_3R over H_4R selectivity for imidazoles has been widely documented,^{16,17,27,28} while imidazole-containing molecules with H_4R over H_3R selectivity appear more scarce. In two reports, 4-methylhistamine was identified as an agonist with high H_4R selectivity (>100-fold),^{16,17} while others showed that varying degrees of H_4R selectivity can also be obtained with ligands having the “usual” monosubstituted imidazole ring (1–4, Figure 1).^{27,29–32} Our lab recently disclosed a study aimed at deciphering the factors for H_4R and H_3R affinities in a series of clobenpropit analogues.³³ From these studies, isothiurea 5 emerged as a H_4R agonist with high H_4R affinity ($pK_i = 8.8$) and a 4-fold selectivity over H_3R .

This modest list illustrates the subtle and poorly understood nature of H_4R/H_3R selectivity with monosubstituted imidazoles. In this report, we aim to pinpoint some important molecular determinants capable of inducing selectivity in H_4R/H_3R affinities and, as an expansion, of H_3R/H_4R selectivity. To this end, a [1,2,3]triazole scaffold (compounds 6a–w and 7a–f) proved to be a very suitable platform for pharmacological and computational investigations into the subtle factors that influence the affinities of monosubstituted imidazole ligands for H_3R and especially for H_4R .

RESULTS AND DISCUSSION

Design. At the onset of our studies, we decided to explore “click” chemistry as the key chemical transformation because of its appealing ease and chemoselectivity.^{34,35} More specifically, the Cu(I)-catalyzed coupling of azide and alkyne building blocks was to be our key step affording an *anti*-[1,2,3]triazole element. The modular nature of click chemistry should thus pave the way for rapid and efficient exploration of H_4R and H_3R affinities. We envisioned an initial design based on a “scaffold hopping” approach, and toward this end, we selected burimamide analogues (8) reported by us to have good H_4R affinity (Figure 2).¹⁶ That is, our scaffold contains the [1,2,3]triazole core instead of the thiourea unit but can otherwise be decorated with peripheral

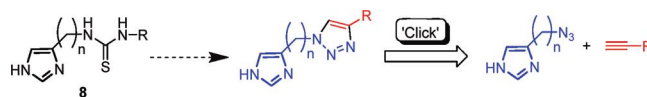
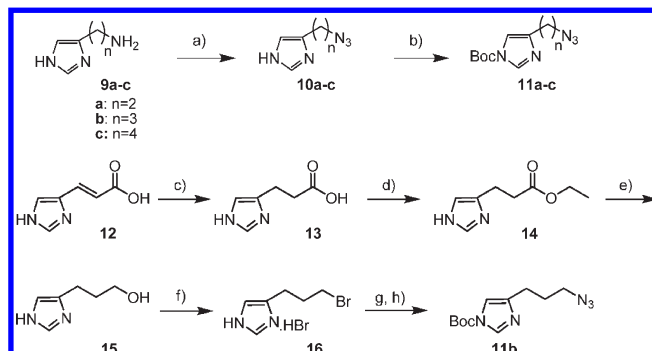


Figure 2. Initial design of the ligands.

Scheme 1. Synthesis of Imidazole-Containing Azides^a



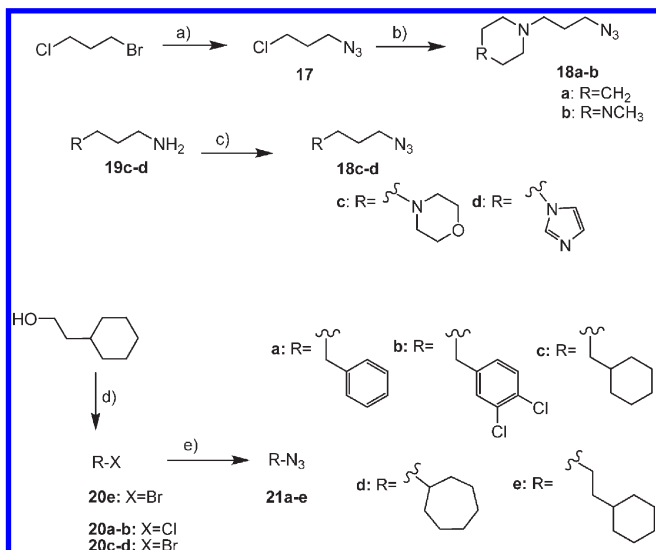
^a Reagents and conditions: (a) TfN_3 , $CuSO_4$, K_2CO_3 , H_2O , DCM, MeOH, rt, 1 day. Yields: **10a**, 92%; **10b**, 88%; **10c**, 47%. (b) Boc_2O , 4-dimethylaminopyridine (DMAP), MeCN, H_2O , dioxane, Et_3N , rt, 1 day. Yields: **11a**, 54%; **11b**, 66%; **11c**, 87%. (c) NH_4CO_2H , Pd/C, MeOH, reflux, 6 h, 99%. (d) H_2SO_4 , EtOH, reflux, 1 d, quant. (e) $LiAlH_4$, THF, rt, overnight, 50%. (f) Aqueous HBr (48%), reflux, 1 d, quant. (g) NaN_3 , H_2O , EtOH, reflux, 1 day. (h) Boc_2O , DMAP, MeCN, H_2O , dioxane, Et_3N , rt, 2 h, 40% over two steps (i.e., from **16**).

groups in a very similar fashion. It is emphasized that the [1,2,3]triazole ring is not a moiety with physiologically relevant basicity ($pK_{HB^+} \leq 1$),³⁶ and hence, many of the envisioned compounds are considered monobasic. It is noted that a recent report shows how click chemistry was applied for non-imidazole H_3R ligands.³⁷

Synthesis. During our structure–activity relationship (SAR) efforts, the design protocol called for the synthesis of several alkyne- and azide-building blocks. The synthesis of these will be discussed in the following sections.

Synthesis of Imidazole-Containing Azides. The synthesis of the required imidazole-containing azides is shown in Scheme 1. Histamine (9a) or its homologues 9b,c were conveniently converted to the corresponding azides 10a–c in one step using a diazo-transfer step (47–92%).³⁸ For reasons explained later, the imidazole ring was Boc-protected, which after column chromatography afforded 11a–c. Large amounts of azide 10b, and hence 11b, could also be obtained by an alternative route. Here, inexpensive urocanic acid (12) is converted in three steps to alcohol 15.³⁹ This is brominated to salt 16 and subjected to a substitution reaction with NaN_3 to give crude 10b with a minor byproduct likely resulting from intramolecular attack by the imidazole ring. Installation of the Boc group and purification afforded 11b (40% from 16).

Synthesis of Non-Imidazole Azides. The synthesis of non-imidazole azides proceeded along conventional synthetic transformations (Scheme 2). 3-Chloro-1-bromopropane was reacted with NaN_3 to give azide 17, which was not isolated but kept as a solution in ether because of the risk of explosion associated with concentrated small organic azides. Reaction of 17 with piperidine or *N*-methylpiperazine yielded azide 18a or 18b, respectively. Amines 19c,d, which are commercially available, were directly

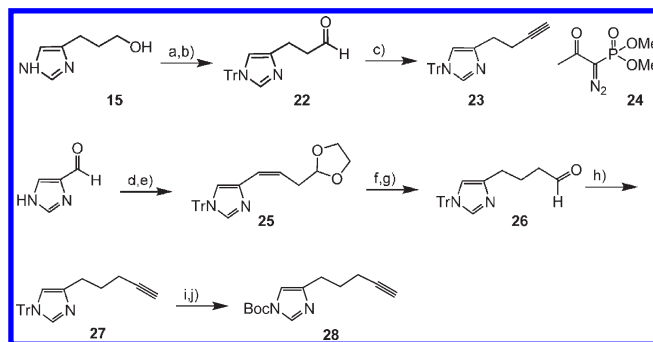
Scheme 2. Synthesis of Non-Imidazole Azides^a

^a Reagents and conditions: (a) NaN_3 , DMSO, rt, 72 h, >90% conversion, kept in ether solution. (b) Amine, NaI, Na_2CO_3 , MeCN, reflux, 24 h. Yields: **18a**, 27%; **18b**, 32%. (c) NaN_3 , CuSO_4 , K_2CO_3 , H_2O , DCM, MeOH, rt, 1 d. Yields: **18c**, 76%; **18d**, 85%. (d) Concentrated aq HBr, concentrated H_2SO_4 , reflux, 24 h, 92%. (e) NaN_3 , EtOH or MeOH, reflux, 24 h. Yields: **21a**, 89%; **21b**, 78%; **21c**, 11%; **21d**, 99%; **21e**, 82%.

converted to the corresponding azides **18c,d** by the azide-transfer protocol (76–85%).³⁸ A range of halides, either commercially available (**20a–d**) or prepared from the alcohol precursor (**20e**), were converted to the corresponding azides **21a–e** by reaction with NaN_3 .

Synthesis of Imidazole-Containing Alkynes. Alkyne **23** has been reported before.⁴⁰ Its preparation starts with the synthesis of aldehyde **22**, itself obtained by tritylation of alcohol **15** followed by a Swern reaction (Scheme 3). However, the reported⁴⁰ Corey–Fuchs protocol on **22** (i.e., CBr_4 , PPh_3 followed by $n\text{-BuLi}$) in our hands failed when attempted on a large scale. Hence, we resorted to a convenient one-step protocol using dimethyl (1-diazo-2-oxopropyl)phosphonate (**24**).⁴¹ This afforded alkyne **23** in high yield (90%). For the longer-chain alkyne homologue of (un)protected **23**, we sought to apply a similar sequence as for **23**. The required aldehyde **26** was prepared through modification of a reported procedure.⁴² It involves a Wittig reaction to give **25** followed by hydrogenation and aldehyde deprotection. Gratifyingly, aldehyde **26** smoothly underwent the one-pot alkylation procedure with phosphonate **24** to give a 79% yield of **27**. A required switch of protecting groups (vide infra) afforded building block **28**.

Synthesis of Non-Imidazole Alkynes. Aminoalkynes **29a,b** were obtained by alkylation with propargyl bromide (Scheme 4). Alkynes **30a–h** are commercially available, whereas **30i,j** require prior synthesis. Methyl-substituted alkyne **30i** was obtained in racemic form following an adapted literature procedure.⁴³ This involves the LiCuI_2 -induced reaction between a Grignard reagent and the propargylic mesylate **31** reportedly through the intermediacy of a propargylic iodide.⁴³ For 3-cycloheptylpropyne (**30j**), we used a methoxyallene-based synthetic strategy described for **30d**⁴⁴ and successfully obtained **30j** by switching to $c\text{-HepMgBr}$. The volatility and very low polarities of both **30i,j** and associated

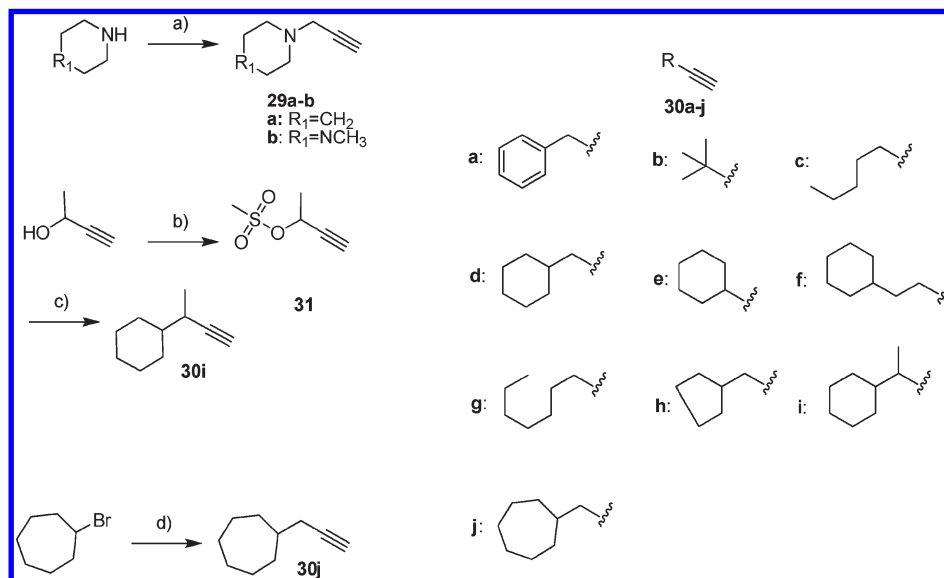
Scheme 3. Synthesis of Imidazole-Containing Alkynes^a

^a Reagents and conditions: (a) Ph_3CCl , Et_3N , DMF, rt, 2 h. (b) [1] Oxalyl chloride, DMSO, DCM, -78°C , 10 min; [2] alcohol, -78°C , 10 min; [3] Et_3N , 39% from **15**. (c) Phosphonate **24**, K_2CO_3 , MeOH, rt, 4 h, 90%. (d) Ph_3CCl , Et_3N , DMF, rt, 4 h. (e) 2-(1,3-Dioxolan-2-yl)-ethyltriphenylphosphonium bromide, $n\text{-BuLi}$, THF, rt, 18 h, 51% over two steps. (f) H_2 , Pd/C, MeOH, EtOH, rt, 72 h. (g) 2 N HCl, acetone, rt, 1 day, quantitative yield from **25**. (h) Phosphonate **24**, K_2CO_3 , MeOH, rt, 4 h, 79%. (i) Concentrated aq HCl, MeOH, H_2O , reflux, 1 h. (j) Boc_2O , MeCN, H_2O , dioxane, Et_3N , rt, 1 day, 60% from **27**.

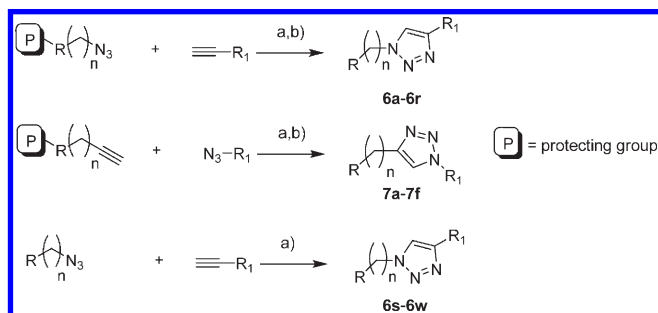
byproducts (e.g., allenes) did not bode well for purification, and we opted to continue with the click reaction using impure **30i,j**.

Fusion of Alkynes and Azides to Final [1,2,3]Triazoles. The syntheses of the final receptor ligands were completed by a Cu-catalyzed click reaction between the azides and alkynes followed, where applicable, by a deprotection (Scheme 5). While the click reaction is an extremely attractive and widely applicable tool and has without doubt also lived up to this reputation in our research, it is of interest to note that we encountered two unusual problems in our early attempts using alkyne **30a** and azide **10a**. The click reaction between **30a** and **10a** under standard conditions (cat. Cu(II) , sodium ascorbate, air, $t\text{-BuOH}/\text{H}_2\text{O}$)³⁴ proceeded very sluggishly and with formation of several undesired products. Qualitative TLC experiments with model reagents shed light on possible reasons for this. First, subjecting **30a** to the click conditions with *but also without* model azide **21a** gave several products more polar than **30a**. This led to the hypothesis that **30a** is oxidized by Cu(II) . In line with this hypothesis we found that keeping the amount of Cu(II) minimal with respect to Cu(I) , either by using strictly deoxygenated conditions or by using large amounts of reducing factor (sodium ascorbate), led to a successful click reaction between **30a** and **21a**. Even so, application of these improved conditions to **30a** and azide **10a** led to a clean but still unacceptably slow reaction. A similar effect was observed for the reaction of **30a** and model **21a** in the presence of stoichiometric amounts of non-azidoimidazole **15**. It was thought that the imidazole group complexes Cu(II) and thereby reduces the amount of active catalyst. We took this hurdle by increasing the amount of Cu catalyst while simultaneously reducing the complexing potential of the imidazole ring by use of the electron-withdrawing protecting group Boc.⁴⁵ This had the added bonus of easier purification of any protected click intermediates.

For practical reasons, all discussed remedies were successfully combined into one general protocol consisting of the use of 1–20 mol % CuSO_4 , 10–200 mol % sodium ascorbate, strict N_2 atmosphere, and Boc-protected imidazole rings (Scheme 5). Interestingly, in retrospect the O_2 removal and reduction of

Scheme 4. Synthesis of Non-Imidazole Alkynes^a

^a Reagents and conditions: (a) propargyl bromide, Cs_2CO_3 , acetone, 20 h, rt. Yields: **29a**, 26%; **29b**, nd. (b) MeSO_2Cl , Et_3N , CH_2Cl_2 , 3 h, 0 °C, 95%. (c) [1] LiI , CuI , THF; [2] mesylate **31**, 2 h, rt; [3] $c\text{-HexMgCl}$, -70 °C, <1 min; [4] sat. aq NH_4Cl , -70 °C, yield: nd. (d) [1] Mg , THF, rt \rightarrow 40 °C, 3.5 h; [2] CuI , methoxyallene, 10 °C, 40 min; [3] rt, 12 h, yield: nd. nd = not determined.

Scheme 5. Synthesis of the Final [1,2,3]Triazoles^a

^a Reagents and conditions: (a) $\text{CuSO}_4 \cdot 5\text{H}_2\text{O}$ (1–20 mol %), sodium ascorbate (10–200 mol %), strict N_2 atmosphere, $t\text{-BuOH}/\text{H}_2\text{O}$, rt, 4–72 h. (b) TFA, DCM, rt, 2–4 h. Except for **7d**: aq HCl, MeOH, reflux, 1 h.

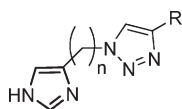
electron density in the imidazole ring by Boc installation may have very well prevented a recently disclosed problem, i.e., the aerobic oxidation of imidazole rings under click conditions lacking stabilizing ligands.⁴⁶ The synthesis of “inverted” triazoles **7a–c,e,f** generally proceeded more smoothly compared to that of the imidazole-containing members of the **6** series. In such cases, amounts of Cu and ascorbate could be reduced. Noteworthy, however, is the click reaction leading to **7d** (i.e., with **23**) which proceeded very sluggishly. This being the only instance where a trityl-protecting group was used instead of a Boc, it appears to reconfirm the importance of reducing the electron density on the imidazole ring and is the reason why a protecting group switch was applied (from **27** to **28**) when we embarked on the longer-chain homologues **7a–c,e,f**.

Any Boc group was deprotected using trifluoroacetic acid (TFA) to give the final compounds. The exception was compound **7d**, for which the trityl group was removed with refluxing HCl. Details for all click reactions and deprotections can be

found in the Supporting Information, including 2D NMR evidence for selected compounds concerning the correct regiochemistry of the [1,2,3]triazole.

Pharmacology. As can be seen in Figure 2, our final compounds can be divided into four parts: an imidazole, a spacer, the [1,2,3]triazole, and the peripheral R group. We started by inspecting the spacer length with the aid of benzyl-substituted derivatives **6a–c**. H_3R and H_4R affinities were measured by radioligand displacement assays using [^3H]N ^{α} -methylhistamine and [^3H]histamine as radioligand, respectively.^{16,21} Histamine and thioperamide were used as controls. The results (Table 1) reveal that the $n = 3$ spacer length is the most attractive for H_4R affinity (**6b**, $\text{pK}_i = 6.74$), albeit that the same held true for H_3R affinity. Using this finding, we next scanned a selected set of aliphatic and polar peripheral R groups that included the known preferred H_4R element 4-methylpiperazine (**6d–g**).²⁴ This led to the conclusion that H_4R affinity benefits best from an aliphatic group R and that, interestingly, **6f** and **6g** provided a first glimpse into $\text{H}_4\text{R}/\text{H}_3\text{R}$ selectivity. The aliphatic group therefore became our point of focus.

Remarkably, H_4R affinity and selectivity got a large boost when a cyclohexylmethyl group was installed (**6h**, $\text{pK}_i(\text{H}_4\text{R}) = 8.08$, $\text{pK}_i(\text{H}_3\text{R}) = 6.90$), prompting us to interrogate this specific group in a detailed SAR study (Table 2). The optimal spacer length of $n = 3$ for H_4R affinity was reinforced (**6h–j**), and spacer lengths of $n = 1$ or $n > 4$ were therefore not pursued. A striking reversal in $\text{H}_4\text{R}/\text{H}_3\text{R}$ selectivity upon simple spacer shortening (compare **6h** to **6i**) was observed. Additional SAR studies on the cyclohexylmethyl moiety showed that methylene removal (**6k**) or insertion (**6l**) and ring-opening (**6m**) all led to compromised H_4R affinity. A sterically more subtle exercise, i.e., methylene substitution to *rac*-**6n**, still afforded good affinity (H_4R $\text{pK}_i = 7.67$), but the $\text{H}_4\text{R}/\text{H}_3\text{R}$ selectivity was reduced by a factor ~ 5 . Ring enlargement to a cycloheptyl (**6o**) also led to a substantial drop in H_4R affinity and H_4/H_3 selectivity. Ring contraction, on the other hand, gave a compound with H_4R affinity and selectivity

Table 1. H₃R and H₄R Affinities of Compounds with Varying Triazole Substituents

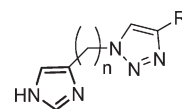
#	n	R	pK _i H ₄ R ± SEM ^a	pK _i H ₃ R ± SEM ^a
Histamine	-	-	7.92 ± 0.07	7.93 ± 0.03
Thioperamide	-	-	7.20 ± 0.06	7.53 ± 0.01
6a	2		5.94 ± 0.03	6.42 ± 0.02
6b	3		6.74 ± 0.09	7.09 ± 0.02
6c	4		6.04 ± 0.05	6.23 ± 0.04
6d	3		5.74 ± 0.01	6.42 ± 0.02
6e	3		4.82 ± 0.04	5.57 ± 0.02
6f	3		7.00 ± 0.06	6.72 ± 0.02
6g	3		7.17 ± 0.04	6.98 ± 0.05

^a Homogenates of human embryonic kidney (HEK) 293T cells, stably expressing either the human H₃R or the human H₄R, were used for determining ligand affinities for H₃R and H₄R with [³H]N^α-methylhistamine and [³H]histamine as radioligand, respectively. Histamine and thioperamide are reference compounds. Measurements shown are the mean of at least three experiments.

matching those of **6h** (**6p**, pK_i(H₄R) = 8.10, pK_i(H₃R) = 7.04). Last, as a final confirmation of the n = 3 spacer length, the best compounds from this mini-SAR (i.e., *rac*-**6n** and **6p**) were subjected to spacer-shortening, affording almost a 100-fold drop in affinity (*rac*-**6r**, **6q**).

Evidently, the nature of the cycloaliphatic group must meet very strict steric demands, as no manipulation on **6h** improved on H₄R affinity. Bearing in mind that analogues of **6h** with N-atoms inserted (i.e., **6d** and **6e**, Table 1) led to dramatic loss of H₄R affinity, the collective data imply that a complementary lipophilic pocket in H₄R is targeted with high steric precision, most notably in **6h** and **6p**. In contrast to this sensitivity associated with H₄R affinity, corresponding H₃R affinities remain strikingly similar in the SAR (Table 2) irrespective of the SAR manipulation involved (spacer shortening or elongation, methylene substitution, ring-contraction or -expansion or -opening). This puts forward the peripheral cycloaliphatic group as an excellent handle to modulate H₄R/H₃R selectivity. Indeed, **6h** and **6p** display H₄R/H₃R selectivities that are noteworthy for monosubstituted imidazoles.

We were interested to see to what extent the central [1,2,3]triazole unit contributes to the observed H₄R affinities.

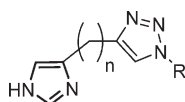
Table 2. H₃R and H₄R Affinities of Compounds with Aliphatic Triazole Substituents^d

#	n	R	pK _i H ₄ R ± SEM ^a	pK _i H ₃ R ± SEM ^a	H ₄ R/H ₃ R ^c
6h	3		8.08 ± 0.06	6.90 ± 0.01	15.2
6i	2		6.11 ± 0.05	7.12 ± 0.06	0.10
6j	4		6.56 ± 0.07	6.49 ± 0.01	1.18
6k	3		7.05 ± 0.03	7.15 ± 0.01	0.80
6l	3		6.85 ± 0.02	7.44 ± 0.03	0.26
6m	3		6.34 ± 0.02	7.01 ± 0.06	0.21
6n ^b	3		7.67 ± 0.07	7.22 ± 0.06	2.82
6o	3		7.26 ± 0.03	6.95 ± 0.05	2.04
6p	3		8.10 ± 0.06	7.04 ± 0.01	11.5
6q	2		6.23 ± 0.02	6.94 ± 0.03	0.20
6r ^b	2		5.94 ± 0.08	7.12 ± 0.08	0.07

^a Homogenates of human embryonic kidney (HEK) 293T cells, stably expressing either the human H₃R or the human H₄R, were used for determining ligand affinities for H₃R and H₄R with [³H]N^α-methylhistamine and [³H]histamine as radioligand, respectively. Measurements shown are the mean of at least three experiments. ^b Measured as racemic mixture. ^c Defined as the K_i for H₄R divided by the K_i for H₃R. ^d Results of reference compounds are given in Table 1.

Toward this end, we swapped the alkyne and azide functional groups of selected combinations, giving the alternative [1,2,3]-triazole fusion product shown in Scheme 5 (**7a–f**, Table 3). Decoration with benzyl groups (**7a,b**) reduced the H₄R affinity compared to benzyl isomer **6b**. Likewise, a ~10-fold reduction of H₄R affinity was observed when the cyclohexylmethyl-group was installed (compare **7c** to **6h**). Nevertheless, within a mini-SAR on **7c** involving spacer shortening, methylene insertion, and ring-shift (**7d–f**), the cyclohexylmethyl group was still preferred for H₄R affinity. It stands to reason that the **7** series is targeting the same H₄R pocket as the **6** series does. Nonetheless, the consistent decrease in affinity of **7a,c,e** compared to **6b,h,l**, respectively,

Table 3. H₄R Affinities of Compounds with an “Inverted” Triazole Core^c



#	n	R	pK _i H ₄ R ± SEM ^a
7a	3		6.35 ± 0.04
7b	3		6.35 ± 0.02
7c	3		7.10 ± 0.02
7d ^b	2		6.23 ± 0.04
7e	3		6.42 ± 0.03
7f	3		6.60 ± 0.05

^a Homogenates of human embryonic kidney (HEK) 293T cells, stably expressing the human H₄R, were used for determining ligand affinities for H₄R with [³H]histamine as radioligand. Measurements shown are the mean of at least three experiments. ^b Tested as the dihydrochloride salt. ^c Results of reference compounds are given in Table 1.

indicates that it does so in a less efficient manner as a result of inverting the [1,2,3]triazole core. Hence, this scaffold was not pursued further.

The functional activities of **6h** and **6i** on both H₄R (Figure 3A) and H₃R (Figure 3B) were tested in a CRE (cAMP response element) luciferase reporter gene assay with agonist histamine and inverse agonist thioperamide as controls. Figure 3 clearly shows that **6h** and **6i** display agonistic behavior on H₄R, with the corresponding pEC₅₀ values being 9.0 ± 0.1 and 6.8 ± 0.1, respectively (*n* = 3). Noteworthy in this respect is the absence of a second basic site in these agonists (triazole pK_{HB+} ≤ 1),³⁶ which is frequently associated with H₄R agonism.^{15,16,33} While **6i** is also an agonist on H₃R (pEC₅₀ = 6.6 ± 0.1), we found that **6h** is unable to evoke a response on H₃R. These data point toward a spacer-dependent agonism/antagonism switch for H₃R in this class of compounds.

The striking sensitivity with H₄R affinities and contrasting insensitivity with H₃R affinities in the **6** series led us to investigate whether the same versatile [1,2,3]triazole scaffold could be used to make H₃R-selective ligands (Table 4). The starting point was compound **6d** which displays dramatically reduced H₄R affinity (pK_i = 5.7) compared to **6h** with, however, an accompanying smaller drop in H₃R affinity (Table 1). It was hypothesized that H₃R affinity could be increased more than the H₄R affinity by

replacement of the imidazole by alternative basic groups.⁴ To confirm this hypothesis, we first used the best H₄R binder **6h** as a case. Replacement of the C-linked imidazole in **6h** by an N-linked imidazole (**6s**) proved to be fruitless. However, within the explored replacements by cyclic amines (**6t–v**), ligands **6u,v** pushed the pK_i for H₄R below 5.0 while H₃R affinity could be largely maintained with respect to **6h**, especially so for piperidine **6v**. With the latter finding at hand, we next returned to starting point **6d** and replaced its imidazole group by a piperidine (affording **6w**). Gratifyingly, **6w** displayed a H₃R affinity of 6.92 with a H₃R/H₄R selectivity >300. Indeed, the double-piperidine motif is not uncommon among other H₃R ligands reported in the literature.^{47,48}

In all, by replacing the peripheral imidazole and cyclohexyl units in H₄R-selective compound **6h** by two piperidines (i.e., **6w**), we were able to maintain the exact same H₃R affinity but induced a concomitant drop in H₄R affinity by almost a factor 5000. As a whole, this reinforces the notion that H₃R is generally forgiving toward decoration of our [1,2,3]triazole based scaffold while H₄R affinities are dramatically affected. Future studies could address the question of whether these observations extend from human H₄R and H₃R to those of other species.

Structure-Based Rationalization of Structure–Activity Relationships. Molecular modeling studies based on three-dimensional H₃R and (previously validated⁴⁹) H₄R receptor models and ligand–receptor interaction fingerprint analysis^{50,51} of docking simulations⁵² (described in the Supporting Information) were used to explain two illustrative selectivity switches.

Known selective H₄R agonists 4-methylhistamine¹⁶ and OUP-16 (**1**)²⁹ could be accommodated in the H₄R model while forming H-bonds with both essential negatively ionizable residues D3.32 and E5.46^{53,54} simultaneously (see Supporting Information Figure S2). In the H₃R model, on the other hand, no binding modes of 4-methylhistamine and **1** could be generated, which satisfied both essential H-bond interactions⁵⁵ (see Supporting Information Figure S2), demonstrating the suitability of the H₃R and H₄R models to rationalize H₄R over H₃R selectivity.

We used the same docking approach⁵⁶ to propose binding modes for the H₄R selective agonist **6h** in the H₃R and H₄R receptor models (Figure 4A,B). The imidazole group of **6h** forms an H-bond to D3.32 in H₃R (Figure 4A) and H₄R (Figure 4B) receptors. This binding mode is in line with earlier site-directed mutagenesis (SDM) studies indicating the essential role of D3.32 in ligand binding in H₃R⁵⁵ and H₄R.^{53,54} Mutation of E5.46, another conserved negatively charged residue in H₃R and H₄R binding pockets, diminishes histamine binding^{54,55} but does not affect binding of iodoproxyfan (which does not bind to the D3.32 mutant in H₃R).⁵⁵ Altogether this suggests that the imidazole headgroup of iodoproxyfan interacts with D3.32.⁵⁷ In H₃R, **6h** accepts an H-bond from T6.52 to the triazole moiety while accommodating its lipophilic cyclohexyl ring into the hydrophobic pocket between TM helices 3 (A3.40), 5 (F5.47), and 6 (F6.44, W6.48) (Figure 4A). In H₄R, the smaller T6.55 residue (M6.55 H₃R) allows the triazole group of **6h** to approach TMS and accept an H-bond from S5.42 (Figure 4B).

Our receptor models can be used to rationalize the overall H₄R over H₃R selectivity drop from **6h** to **6w** by a factor ~5000 (Table 4) that can be achieved by our [1,2,3]triazole compounds. Modification of the imidazole head to a piperidine or piperazine group has a dramatic effect on the affinity for H₄R because the intramolecular H-bond interaction between D3.32 and Q7.42

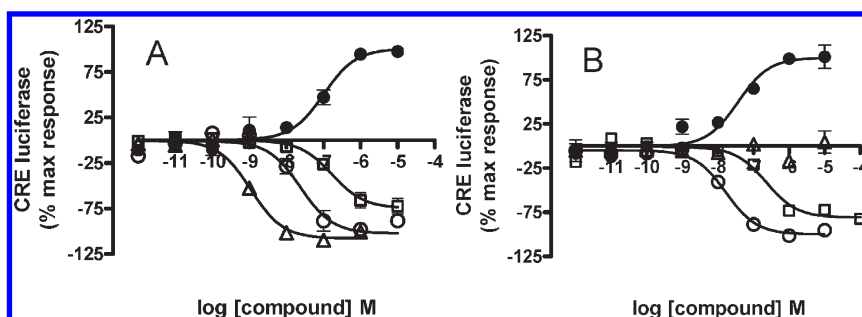
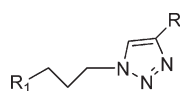


Figure 3. Functional activity of **6i** and **6h** on hH₄R (A) and hH₃R (B). Effect of histamine (○), thioperamide (●), **6i** (□), and **6h** (△) on 1 μ M forskoline-stimulated HEK293T cells transiently expressing CRE luciferase and hH₄R or hH₃R was measured. Agonist histamine ($pEC_{50} = 7.6 \pm 0.1$ (H₄R), 7.8 ± 0.1 (H₃R)) and inverse agonist thioperamide ($pEC_{50} = 7.1 \pm 0.2$ (H₄R), 7.4 ± 0.2 (H₃R)) were used as controls, and their values were set at -100% and 100% , respectively. Graphs shown are pooled data from at least three independently performed experiments. Error bars indicate SEM values.

Table 4. H₃R and H₄R Affinities of Compounds with Varying Peripheral Groups^d



#	R ₁	R	pK _i H ₄ R \pm SEM ^a	pK _i H ₃ R \pm SEM ^a	H ₄ R/H ₃ R ^b
6h			8.08 \pm 0.06	6.90 \pm 0.01	15.2
6d			5.74 \pm 0.01	6.42 \pm 0.02	0.21
6s			4.66 \pm 0.09	5.20 \pm 0.01	0.29
6t ^c			5.32 \pm 0.04	4.73 \pm 0.24	3.89
6u			4.68 \pm 0.12	6.10 \pm 0.03	0.04
6v			4.95 \pm 0.10	6.31 \pm 0.11	0.04
6w ^c			4.41 \pm 0.11	6.92 \pm 0.02	0.003

^a Homogenates of human embryonic kidney (HEK) 293T cells, stably expressing either the human H₃R or the human H₄R, were used for determining ligand affinities for H₃R and H₄R with [³H]N ^{α} -methylhistamine and [³H]histamine as radioligand, respectively. Measurements shown are the mean of at least three experiments. ^b Defined as the K_i for H₄R divided by the K_i for H₃R. ^c Tested as the fumarate salt. ^d Results of reference compounds are given in Table 1.

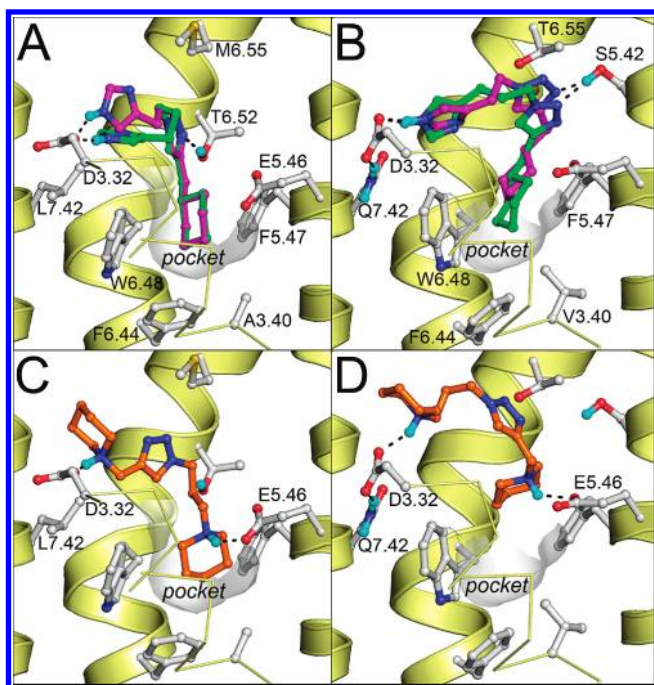


Figure 4. Binding modes of **6h** (green carbon atoms) and **6i** (magenta atoms) in H_3R (A) and H_4R (B) and **6w** (orange atoms) in H_3R (C) and H_4R (D) receptor models. The backbones of TM helices 5, 6, and 7 are represented by yellow ribbons, and part of TM3 is shown as ribbon (the top of the helix is not shown for clarity). Important binding residues are depicted as ball-and-sticks with gray carbon atoms. The bottom of the lipophilic binding pocket between TM helices 3, 5, and 6 is displayed as a gray surface. Oxygen, nitrogen sulfur, and hydrogen atoms are colored red, blue, yellow, and cyan, respectively. H-Bonds are depicted by black dotted lines.

(L7.42 in H_3R) in H_4R does not allow binding of a large moiety between TM3 and TM7 as exemplified for compound **6w** (Figure 4C). Reorientation of the ligand shifts the other piperidine ring of **6w** even further out of the apolar binding pocket of H_4R . Docking simulations of **6w** in H_3R suggest that the two piperidine rings cannot be simultaneously accommodated in the apolar binding pockets between D3.32 and L7.42 and between TM3, TM5, and TM6 (Figure 4D). This is, however, compensated by favorable ionic interactions with D3.32 and E5.46.

The most intriguing H_4R/H_3R selectivity switch observed in our SAR, however, was the 151-fold change in receptor selectivity from compound **6h** (H_4R over H_3R selectivity, 15.1) to **6i** (H_4R over H_3R selectivity, 0.1) by decreasing the linker length with just a single C–C bond (Table 2). Compounds **6h** and **6i** adopt similar binding modes in the H_3R receptor model (Figure 4A), in line with the very similar binding affinities of **6h** and **6i** for H_3R (Table 2). In H_4R , however, compound **6h** can accommodate its cyclohexyl ring significantly deeper in the hydrophobic pocket between TM helices 3 (V3.40), 5 (F5.47), and 6 (F6.44, W6.48) than **6i** (Figure 4B), providing a plausible explanation for its higher affinity for H_4R (Table 2). Interestingly, mutation of A3.40 into a valine residue (the corresponding residue in H_4R at this position) increases H_3R affinity for neutral imidazole containing ligands,⁵⁸ supporting the important role of this hydrophobic pocket in H_4R over H_3R selectivity of **6h** (Table 2), as suggested by our modeling studies.

CONCLUSION

This paper describes compounds containing a [1,2,3]triazole core, obtained by Cu(I)-catalyzed fusions of an alkyne and azide (“click reaction”). Some synthetic hurdles were encountered concerning imidazole moieties and an oxidizable alkyne. These issues were successfully counteracted by applying several remedies: O_2 removal, increase in amount of ascorbate, decrease of electron density on the imidazole, and an increase in amount of catalysts. The general skeleton thus synthesized consists of an imidazole, a spacer, the [1,2,3]triazole, and the peripheral R group. In terms of decoration of the [1,2,3]triazole scaffold, H_4R affinities proved remarkably sensitive while H_3R affinities were strikingly insensitive, allowing a spectrum of H_4R/H_3R selectivities to be obtained. With subtle changes in aliphatic group, H_4R -agonist **6h** was obtained which boosted high H_4R affinity ($pK_i = 8.08$) and a good H_4R/H_3R selectivity of 15, noteworthy for a monosubstituted imidazole compound. In contrast, a replacement of both peripheral groups by piperidines led to compound **6w** with good H_3R affinity ($pK_i = 6.92$) and excellent H_3R/H_4R selectivity (320). Molecular modeling studies were used to address the role of the cycloalkylmethyl group, to inspect receptor–ligand interactions when two peripheral piperidines are installed, and to explain a key selectivity switch upon spacer shortening. In all, the versatile [1,2,3]triazole core has proven to be a useful tool scaffold to investigate the at times intriguingly subtle differences between affinities for H_4R and H_3R .

EXPERIMENTAL SECTION

General Remarks. Given the possibility of explosions, caution should be exercised when working with organic azides, especially those with low molecular weight. Unless reported otherwise, all chemicals were from Aldrich. THF, toluene, and CH_2Cl_2 were freshly distilled from CaH_2 . All other solvents were used as received. Unless indicated otherwise, all reactions were carried out under an inert atmosphere. TLC analyses were performed with Merck F254 alumina silica plates using UV visualization or staining. Column purifications were carried out manually using Silicycle Ultra Pure silica gel or automatically using the Biotage equipment. All HRMS spectra were recorded on Bruker micrOTOF mass spectrometer using ESI in positive ion mode. The 1H , ^{13}C , and 2D NMR spectra were recorded on a Bruker 200, 250, 400, or 500 MHz spectrometer. Depending on the exact conditions, 1H and/or ^{13}C signals for the protons and carbons of unprotected imidazole rings were not or only partially visible. On a few occasions, high-temperature NMR was shown to restore the visibility of these signals (see data for **6h** and **6p**). Infrared spectra were recorded on a Galaxy series FT-IR 6030. Melting points were taken using the Stanford Research Systems Optimelt apparatus, and values given are uncorrected. Elemental analysis results were recorded at Mikroanalytisches Labor Pascher (Remagen-Bandorf, Germany). Systematic names for molecules according to IUPAC rules were generated using the Chemdraw AutoNom program. Unless specified otherwise, all compounds have a purity of $\geq 95\%$. This was determined using a Shimadzu HPLC/MS workstation with a LC-20AD pump system, SPD-M20A diode array detection, and a LCMS-2010 EV liquid chromatograph mass spectrometer. The buffer mentioned is a 0.4% (w/v) NH_4HCO_3 solution in water, adjusted to pH 8.0 with NH_4OH . The column used is an Xbridge C18 5 μm column (100 mm \times 4.6 mm). Compound purities were calculated as the percentage peak area of the analyzed compound by UV detection at 230 nm. Solvents used in this paragraph were the following: solvent B = 90% MeCN–10% buffer; solvent A = 90% water–10% buffer. The analysis was conducted using a flow rate of 1.0 mL/min, start 5% B, linear gradient to 90% B in 8 min, then 0.5 min at 90% B, then 6.5 min at

5% B, total run time of 15 min. The occasional fumarate counterion is also visible by UV. For compound **6w**, purity is >95% as determined by elemental analysis.

General Procedure for Synthesis of 6a–w and 7a–f. In a round-bottom flask, the azide and alkyne were mixed with the indicated volume of *t*-BuOH/H₂O. Then the indicated amount of sodium ascorbate was added as a solid and a septum was placed on the flask. The mixture was degassed by bubbling N₂ through the solution for 5 min using a needle. The indicated amount of a solution of CuSO₄·5H₂O in water (0.3 M) was added with the aid of a syringe. The mixture was briefly degassed again by bubbling N₂ through for 2 min. The mixture was stirred under a N₂ atmosphere and at room temperature for the indicated time. One of three workup/deprotection protocols (see Supporting Information) was subsequently used to provide **6a–w** and **7a–f**.

1-(3-(1*H*-imidazol-4-yl)propyl)-4-(cyclohexylmethyl)-1*H*-1,2,3-triazole (6h). The general procedure was followed using azide **11b** (100 mg, 0.4 mmol), alkyne **30d** (64 μ L, 0.44 mmol), water (2 mL), *t*-BuOH (2 mL), sodium ascorbate (174 mg, 0.88 mmol), CuSO₄ solution (0.3 M, 0.27 mL, 0.08 mmol), and a reaction time of 1 night. Subsequently, protocol no. 2 (see Supporting Information) was used including (a) column chromatography on the intermediate (6:2:1 hexane/DCM/TEA) and (b) deprotection using TFA (1 mL), DCM (1 mL), and a reaction time of 2 h. This gave the product as a white solid (60 mg, 55%). ¹H NMR (CDCl₃): δ = 9.33 (br, 1H), 7.61 (br, 1H), 7.28 (s, 1H), 6.84 (br, 1H), 4.33 (t, 2H, *J* = 6.9 Hz), 2.62 (t, 2H, *J* = 6.3 Hz), 2.54 (d, 2H, *J* = 6.8 Hz), 2.22 (p, 2H), 1.73–1.48 (m, 6H), 1.28–1.04 (m, 3H), 1.03–0.84 (m, 2H); imidazole protons and N–H are very broad. ¹³C NMR (CDCl₃): δ = 146.34, 120.98, 48.65, 37.44, 32.80, 32.32, 29.56, 26.00, 25.43, 23.18; imidazole carbons are difficult to detect. Peaks were sharpened substantially in DMSO at higher temperature: ¹H NMR (DMSO-*d*₆, 350 K): δ = 11.60 (v br, 1H), 7.75 (s, 1H), 7.49 (s, 1H), 6.77 (s, 1H), 4.33 (t, 2H, *J* = 7.1 Hz), 2.54–2.49 (m, 4H), 2.12 (p, 2H), 1.72–1.53 (m, 6H), 1.29–1.10 (m, 3H), 1.03–0.91 (m, 2H). HR-MS: [M + H]⁺ C₁₅H₂₄N₅ calcd, 274.2026; found, 274.2015. The Supporting Information contains graphical descriptions on 2D NMR analysis and a LC–MS chromatogram.

1-(3-(1*H*-imidazol-4-yl)propyl)-4-(cyclopentylmethyl)-1*H*-1,2,3-triazole (6p). The general procedure was followed using azide **11b** (100 mg, 0.4 mmol), alkyne **30h** (52 mg, 0.48 mmol), water (2 mL), *t*-BuOH (2 mL), sodium ascorbate (174 mg, 0.88 mmol), CuSO₄ solution (0.3 M, 0.27 mL, 0.08 mmol), and a reaction time of 1 night. Subsequently, protocol no. 2 (see Supporting Information) was used including (a) column chromatography on the intermediate (6:2:1 hexane/DCM/TEA) and (b) deprotection using TFA (1 mL), DCM (1 mL), and a reaction time of 2 h. This gave the product as a white oily solid (52 mg, 50%). ¹H NMR (CDCl₃): δ = 8.41 (br, 1H), 7.57 (s, 1H), 7.30 (s, 1H), 6.80 (s, 1H), 4.33 (t, 2H, *J* = 7.0 Hz), 2.68 (d, 2H, *J* = 7.2 Hz), 2.60 (t, 2H, *J* = 7.1 Hz), 2.21 (p, 2H), 2.19–2.03 (m, 1H), 1.81–1.64 (m, 2H), 1.65–1.42 (m, 4H), 1.27–1.09 (m, 2H). ¹³C NMR (CDCl₃): δ = 147.42, 135.37, 134.41, 119.83, 116.36, 48.65, 39.47, 32.06, 31.14, 29.58, 24.66, 23.06; imidazole carbons are visible but small. Peaks were sharpened substantially in DMSO at higher temperature: ¹H NMR (DMSO-*d*₆, 350 K): δ = 11.58 (br), 7.77 (s, 1H), 7.48 (s, 1H), 6.76 (s, 1H), 4.33 (t, 2H, *J* = 7.1 Hz), 2.63 (d, 2H, *J* = 7.3 Hz), 2.51 (t, 2H), 2.20–2.04 (m, 3H), 1.79–1.69 (m, 2H), 1.65–1.45 (m, 4H), 1.28–1.17 (m, 2H). HR-MS: [M + H]⁺ C₁₄H₂₂N₅ calcd, 260.1870; found, 260.1862. The Supporting Information contains graphical descriptions on 2D NMR analysis and a LC–MS chromatogram.

■ ASSOCIATED CONTENT

Supporting Information. Procedures for pharmacological assays; molecular modeling procedures; syntheses and

characterization of all compounds; representative 1D, 2D, and high-temperature NMR spectra; and selected LC chromatograms. This material is available free of charge via the Internet at <http://pubs.acs.org>.

■ AUTHOR INFORMATION

Corresponding Author

*Phone: +31-20-5987603. Fax: +31-20-5987610. E-mail: m.wijtmans@vu.nl

■ ACKNOWLEDGMENT

This work was supported by the Top Institute Pharma (Project Number D1.105, the GPCR Forum), The Netherlands Organization for Scientific Research (VENI Grant 700.59.408), and COST Action BM0806. Hans Custers, Tarik Tagherbit, and Kaamar Azizli are acknowledged for technical assistance.

■ ABBREVIATIONS USED

H₄R, histamine H₄ receptor; H₃R, histamine H₃ receptor; GPCR, G protein-coupled receptor; DMAP, 4-dimethylamino-pyridine; TFA, trifluoroacetic acid; HEK, human embryonic kidney; *rac*, racemic; CRE, cAMP response element; SAR, structure–activity relationship; TM, transmembrane; SDM, site-directed mutagenesis; rt, room temperature

■ REFERENCES

- (1) Hough, L. B. Genomics meets histamine receptors: new subtypes, new receptors. *Mol. Pharmacol.* **2001**, *59*, 415–419.
- (2) Arrang, J. M.; Garbarg, M.; Schwartz, J. C. Autoinhibition of brain histamine release mediated by a novel class (H₃) of histamine receptor. *Nature* **1983**, *302*, 832–837.
- (3) Lovenberg, T. W.; Roland, B. L.; Wilson, S. J.; Jiang, X.; Pyati, J.; Huvar, A.; Jackson, M. R.; Erlander, M. G. Cloning and functional expression of the human histamine H₃ receptor. *Mol. Pharmacol.* **1999**, *55*, 1101–1107.
- (4) Celanire, S.; Wijtmans, M.; Talaga, P.; Leurs, R.; de Esch, I. J. Keynote review: histamine H₃ receptor antagonists reach out for the clinic. *Drug Discovery Today* **2005**, *10*, 1613–1627.
- (5) Gemkow, M. J.; Davenport, A. J.; Harich, S.; Ellenbroek, B. A.; Cesura, A.; Hallett, D. The histamine H₃ receptor as a therapeutic drug target for CNS disorders. *Drug Discovery Today* **2009**, *14*, 509–515.
- (6) Wijtmans, M.; Leurs, R.; de Esch, I. Histamine H₃ receptor ligands break ground in a remarkable plethora of therapeutic areas. *Expert Opin. Invest. Drugs* **2007**, *16*, 967–985.
- (7) Sander, K.; Kottke, T.; Stark, H. Histamine H₃ receptor antagonists go to clinics. *Biol. Pharm. Bull.* **2008**, *31*, 2163–2181.
- (8) de Esch, I. J. P.; Thurmond, R. L.; Jongejan, A.; Leurs, R. The histamine H₄ receptor as a new therapeutic target for inflammation. *Trends Pharmacol. Sci.* **2005**, *26*, 462–469.
- (9) Lim, H. D.; Smits, R. A.; Leurs, R.; De Esch, I. J. P. The emerging role of the histamine H₄ receptor in anti-inflammatory therapy. *Curr. Top. Med. Chem.* **2006**, *6*, 1365–1373.
- (10) Hofstra, C. L.; Desai, P. J.; Thurmond, R. L.; Fung-Leung, W. P. Histamine H₄ receptor mediates chemotaxis and calcium mobilization of mast cells. *J. Pharmacol. Exp. Ther.* **2003**, *305*, 1212–1221.
- (11) Ling, P.; Ngo, K.; Nguyen, S.; Thurmond, R. L.; Edwards, J. P.; Karlsson, L.; Fung-Leung, W. P. Histamine H₄ receptor mediates eosinophil chemotaxis with cell shape change and adhesion molecule upregulation. *Br. J. Pharmacol.* **2004**, *142*, 161–171.
- (12) Thurmond, R. L.; Gelfand, E. W.; Dunford, P. J. The role of histamine H₁ and H₄ receptors in allergic inflammation: the search for new antihistamines. *Nat. Rev. Drug Discovery* **2008**, *7*, 41–53.

- (13) Medina, V.; Croci, M.; Crescenti, E.; Mohamad, N.; Sanchez-Jimenez, F.; Massari, N.; Nunez, M.; Cricco, G.; Martin, G.; Bergoc, R.; Rivera, E. The role of histamine in human mammary carcinogenesis: H3 and H4 receptors as potential therapeutic targets for breast cancer treatment. *Cancer Biol. Ther.* **2008**, *7*, 28–35.
- (14) Cowart, M. D.; Altenbach, R. J.; Liu, H.; Hsieh, G. C.; Drizin, I.; Milicic, I.; Miller, T. R.; Witte, D. G.; Wishart, N.; Fix-Stenzel, S. R.; McPherson, M. J.; Adair, R. M.; Wetter, J. M.; Bettencourt, B. M.; Marsh, K. C.; Sullivan, J. P.; Honore, P.; Esbenshade, T. A.; Brioni, J. D. Rotationally constrained 2,4-diamino-5,6-disubstituted pyrimidines: a new class of histamine H4 receptor antagonists with improved druglike-ness and In Vivo efficacy in pain and inflammation models. *J. Med. Chem.* **2008**, *51*, 6547–6557.
- (15) Lim, H. D.; Smits, R. A.; Bakker, R. A.; van Dam, C. M. E.; de Esch, I. J. P.; Leurs, R. Discovery of *S*-(2-guanidylethyl)-isothiourea (VUF 8430) as a potent nonimidazole histamine H-4 receptor agonist. *J. Med. Chem.* **2006**, *49*, 6650–6651.
- (16) Lim, H. D.; Rijn, R. M. v.; Ling, P.; Bakker, R. A.; Thurmond, R. L.; Leurs, R. Evaluation of histamine H₁-, H₂-, and H₃-receptor ligands at the human histamine H₄ receptor: identification of 4-methyl-histamine as the first potent and selective H₄ receptor agonist. *J. Pharmacol. Exp. Ther.* **2005**, *314*, 1310–1321.
- (17) Gbahou, F.; Vincent, L.; Humbert-Claude, M.; Tardivel-Lacombe, J.; Chabret, C.; Arrang, J. M. Compared pharmacology of human histamine H-3 and H-4 receptors: structure–activity relationships of histamine derivatives. *Br. J. Pharmacol.* **2006**, *147*, 744–754.
- (18) Dijkstra, D.; Leurs, R.; Chazot, P.; Shenton, F. C.; Stark, H.; Werfel, T.; Gutzmer, R. Histamine downregulates monocyte CCL2 production through the histamine H-4 receptor. *J. Allergy Clin. Immunol.* **2007**, *120*, 300–307.
- (19) Smith, F. M.; Haskelberg, H.; Tracey, D. J.; Moalem-Taylor, G. Role of histamine H-3 and H-4 receptors in mechanical hyperalgesia following peripheral nerve injury. *NeuroImmunoModulation* **2008**, *14*, 317–325.
- (20) Altenbach, R. J.; Adair, R. M.; Bettencourt, B. M.; Black, L. A.; Fix-Stenzel, S. R.; Gopalakrishnan, S. M.; Hsieh, G. C.; Liu, H.; Marsh, K. C.; McPherson, M. J.; Milicic, I.; Miller, T. R.; Vortherms, T. A.; Warrior, U.; Wetter, J. M.; Wishart, N.; Witte, D. G.; Honore, P.; Esbenshade, T. A.; Hancock, A. A.; Brioni, J. D.; Cowart, M. D. Structure–activity studies on a series of a 2-aminopyrimidine-containing histamine H4 receptor ligands. *J. Med. Chem.* **2008**, *51*, 6571–6580.
- (21) Smits, R. A.; Lim, H. D.; Hanzer, A.; Zuiderveld, O. P.; Guaita, E.; Adami, M.; Coruzzi, G.; Leurs, R.; de Esch, L. J. P. Fragment based design of new H-4 receptor-ligands with anti-inflammatory properties In Vivo. *J. Med. Chem.* **2008**, *51*, 2457–2467.
- (22) Smits, R. A.; de Esch, L. J.; Zuiderveld, O. P.; Broeker, J.; Sansuk, K.; Guaita, E.; Coruzzi, G.; Adami, M.; Haaksma, E.; Leurs, R. Discovery of quinazolines as histamine H4 receptor inverse agonists using a scaffold hopping approach. *J. Med. Chem.* **2008**, *51*, 7855–7865.
- (23) Jablonowski, J. A.; Grice, C. A.; Chai, W. Y.; Dvorak, C. A.; Venable, J. D.; Kwok, A. K.; Ly, K. S.; Wei, J. M.; Baker, S. M.; Dsesai, P. J.; Jiang, W.; Wilson, S. J.; Thurmond, R. L.; Karlsson, L.; Edwards, J. P.; Lovenberg, T. W.; Carruthers, N. I. The first potent and selective non-imidazole human histamine H-4 receptor antagonists. *J. Med. Chem.* **2003**, *46*, 3957–3960.
- (24) Smits, R. A.; Leurs, R.; de Esch, I. J. Major advances in the development of histamine H4 receptor ligands. *Drug Discovery Today* **2009**, *14*, 745–753.
- (25) Varga, C.; Horvath, K.; Berko, A.; Thurmond, R. L.; Dunford, P. J.; Whittle, B. J. R. Inhibitory effects of histamine H-4 receptor antagonists on experimental colitis in the rat. *Eur. J. Pharmacol.* **2005**, *522*, 130–138.
- (26) Thurmond, R. L.; Desai, P. J.; Dunford, P. J.; Fung-Leung, W. P.; Hofstra, C. L.; Jiang, W.; Nguyen, S.; Riley, J. P.; Sun, S. Q.; Williams, K. N.; Edwards, J. P.; Karlsson, L. A potent and selective histamine H-4 receptor antagonist with anti-inflammatory properties. *J. Pharmacol. Exp. Ther.* **2004**, *309*, 404–413.
- (27) Watanabe, M.; Kazuta, Y.; Hayashi, H.; Yamada, S.; Matsuda, A.; Shuto, S. Stereochemical diversity-oriented conformational restriction strategy. Development of potent histamine H-3 and/or H-4 receptor antagonists with an imidazolylcyclopropane structure. *J. Med. Chem.* **2006**, *49*, 5587–5596.
- (28) Łazewska, D.; Więcek, M.; Ligneau, X.; Kottke, T.; Weizel, L.; Seifert, R.; Schunack, W.; Stark, H.; Kieć-Kononowicz, K. Histamine H3 and H4 receptor affinity of branched 3-(1*H*-imidazol-4-yl)propyl *N*-alkylcarbamates. *Bioorg. Med. Chem. Lett.* **2009**, *19*, 6682–6685.
- (29) Hashimoto, T.; Harusawa, S.; Araki, L.; Zuiderveld, O. P.; Smit, M. J.; Imazu, T.; Takashima, S.; Yamamoto, Y.; Sakamoto, Y.; Kurihara, T.; Leurs, R.; Bakker, R. A.; Yamatodani, A. A selective human H-4-receptor agonist: (–)-2-cyano-1-methyl-3-[(2*R*,5*R*)-5-[1*H*-imidazol-4(5*S*)-yl]tetrahydrofuran-2-yl]methylguanidine. *J. Med. Chem.* **2003**, *46*, 3162–3165.
- (30) Igel, P.; Schneider, E.; Schnell, D.; Elz, S.; Seifert, R.; Buschauer, A. *N*(G)-Acylylated imidazolylpropylguanidines as potent histamine H4 receptor agonists: selectivity by variation of the *N*(G)-substituent. *J. Med. Chem.* **2009**, *52*, 2623–2627.
- (31) Igel, P.; Geyer, R.; Strasser, A.; Dove, S.; Seifert, R.; Buschauer, A. Synthesis and structure–activity relationships of cyanoguanidine-type and structurally related histamine H4 receptor agonists. *J. Med. Chem.* **2009**, *52*, 6297–6313.
- (32) Savall, B. M.; Edwards, J. P.; Venable, J. D.; Buzard, D. J.; Thurmond, R.; Hack, M.; McGovern, P. Agonist/antagonist modulation in a series of 2-aryl benzimidazole H₄ receptor ligands. *Bioorg. Med. Chem. Lett.* **2010**, *20*, 3367–3371.
- (33) Lim, H. D.; Istyastono, E. P.; van de Stolpe, A.; Romeo, G.; Gobbi, S.; Schepers, M.; Lahaye, R.; Menge, W. M.; Zuiderveld, O. P.; Jongejan, A.; Smits, R. A.; Bakker, R. A.; Haaksma, E. E.; Leurs, R.; de Esch, I. J. Clobenpropit analogs as dual activity ligands for the histamine H3 and H4 receptors: synthesis, pharmacological evaluation, and cross-target QSAR studies. *Bioorg. Med. Chem.* **2009**, *17*, 3987–3994.
- (34) Rostovtsev, V. V.; Green, L. G.; Fokin, V. V.; Sharpless, K. B. A stepwise Huisgen cycloaddition process: copper(I)-catalyzed regioselective “ligation” of azides and terminal alkynes. *Angew. Chem., Int. Ed.* **2002**, *41*, 2596–2599.
- (35) Kolb, H. C.; Sharpless, K. B. The growing impact of click chemistry on drug discovery. *Drug Discovery Today* **2003**, *8*, 1128–1137.
- (36) Abboud, J.-L. M.; Foces-Foces, C.; Notario, R.; Trifonov, R. E.; Volovodenko, A. P.; Ostrovskii, V. A.; Alkorta, I.; Elguero, J. Basicity of *N*-H- and *N*-methyl-1,2,3-triazoles in the gas phase, in solution, and in the solid state: an experimental and theoretical study. *Eur. J. Org. Chem.* **2001**, 3013–3024.
- (37) Sander, K.; Kottke, T.; Hoffend, C.; Walter, M.; Weizel, L.; Camelin, J. C.; Ligneau, X.; Schneider, E. H.; Seifert, R.; Schwartz, J. C.; Stark, H. First metal-containing histamine H₃ receptor ligands. *Org. Lett.* **2010**, *12*, 2578–2581.
- (38) Lundquist, J. T.; Pelletier, J. C. Improved solid-phase peptide synthesis method utilizing alpha-azide-protected amino acids. *Org. Lett.* **2001**, *3*, 781–783.
- (39) Ganellin, C. R.; Fkyerat, A.; Bang-Andersen, B.; Athmani, S.; Tertiu, W.; Garbarg, M.; Ligneau, X.; Schwartz, J. C. A novel series of (phenoxyalkyl)imidazoles as potent H3-receptor histamine antagonists. *J. Med. Chem.* **1996**, *39*, 3806–3813.
- (40) Ali, S. M.; Tedford, C. E.; Gregory, R.; Handley, M. K.; Yates, S. L.; Hirth, W. W.; Phillips, J. G. Design, synthesis, and structure–activity relationships of acetylene-based histamine H3 receptor antagonists. *J. Med. Chem.* **1999**, *42*, 903–909.
- (41) Meffre, P.; Hermann, S.; Durand, P.; Reginato, G.; Riu, A. Practical one-step synthesis of ethynylglycine synthon from Garner's aldehyde. *Tetrahedron* **2002**, *58*, S159–S162.
- (42) Tozer, M. J.; Buck, I. M.; Cooke, T.; Kalindjian, S. B.; Pether, M. J.; Steel, K. I. omega-(Imidazol-4-yl)alkane-1-sulfonamides: a new series of potent histamine H(3) receptor antagonists. *Bioorg. Med. Chem.* **2002**, *10*, 425–432.
- (43) Bargar, T. M.; Lett, R. M.; Johnson, P. L.; Hunter, J. E.; Chang, C. P.; Pernich, D. J.; Sabol, M. R.; Dick, M. R. Toxicity of pumiliotoxin

251D and synthetic analogs to the cotton pest *heliiothis virescens*. *J. Agric. Food Chem.* **1995**, *43*, 1044–1051.

(44) Fleming, I.; Morgan, I. T.; Sarkar, A. K. The stereochemistry of the vinylogous Peterson elimination. *J. Chem. Soc., Perkin Trans. 1* **1998**, 2749–2763.

(45) In preliminary TLC experiments carried out later, we found that the use of CuBr₂, Cu wire, or the Cu(I) binder 2,2'-biquinoline-4,4'-dicarboxylic acid dipotassium salt all led to much faster reaction between azide **10a** and phenylacetylene, whereas the corresponding conditions with Cu(II)SO₄ still afforded very slow conversion. This was not elaborated upon further, though.

(46) Hong, V.; Presolski, S. I.; Ma, C.; Finn, M. G. Analysis and optimization of copper-catalyzed azide–alkyne cycloaddition for bioconjugation. *Angew. Chem., Int. Ed.* **2009**, *48*, 9879–9883.

(47) Bertoni, S.; Flammini, L.; Manenti, V.; Ballabeni, V.; Morini, G.; Comini, M.; Barocelli, E. In vitro pharmacology at human histamine H3 receptors and brain access of non-imidazole alkylpiperidine derivatives. *Pharmacol. Res.* **2007**, *55*, 111–116.

(48) Apodaca, R.; Dvorak, C. A.; Xiao, W.; Barbier, A. J.; Boggs, J. D.; Wilson, S. J.; Lovenberg, T. W.; Carruthers, N. I. A new class of diamine-based human histamine H3 receptor antagonists: 4-(aminoalkoxy)-benzylamines. *J. Med. Chem.* **2003**, *46*, 3938–3944.

(49) Lim, H. D.; de Graaf, C.; Jiang, W.; Sadek, P.; McGovern, P. M.; Istyastono, E. P.; Bakker, R. A.; de Esch, I. J. P.; Thurmond, R. L.; Leurs, R. Molecular determinants of ligand binding to H4R species variants. *Mol. Pharmacol.* **2010**, *77*, 734–743.

(50) de Graaf, C.; Rognan, D. Selective structure-based virtual screening for full and partial agonists of the beta2 adrenergic receptor. *J. Med. Chem.* **2008**, *51*, 4978–4985.

(51) Marcou, G.; Rognan, D. Optimizing fragment and scaffold docking by use of molecular interaction fingerprints. *J. Chem. Inf. Model.* **2007**, *47*, 195–207.

(52) Korb, O.; Stutzle, T.; Exner, T. E. An ant colony optimization approach to flexible protein–ligand docking. *Swarm Intell.* **2007**, *1*, 115–134.

(53) Shin, N.; Coates, E.; Murgolo, N. J.; Morse, K. L.; Bayne, M.; Strader, C. D.; Monsma, F. J., Jr. Molecular modeling and site-specific mutagenesis of the histamine-binding site of the histamine H4 receptor. *Mol. Pharmacol.* **2002**, *62*, 38–47.

(54) Jongejan, A.; Lim, H. D.; Smits, R. A.; de Esch, I. J.; Haaksma, E.; Leurs, R. Delineation of agonist binding to the human histamine H4 receptor using mutational analysis, homology modeling, and ab initio calculations. *J. Chem. Inf. Model.* **2008**, *48*, 1455–1463.

(55) Uveges, A. J.; Kowal, D.; Zhang, Y.; Spangler, T. B.; Dunlop, J.; Semus, S.; Jones, P. G. The role of transmembrane helix 5 in agonist binding to the human H3 receptor. *J. Pharmacol. Exp. Ther.* **2002**, *301*, 451–458.

(56) Docking poses donating an H-bond to D3.32 with the highest PLANTS score were selected using a protein–ligand interaction fingerprint scoring protocol. The binding modes of the selected docking poses remained stable during short (200 ps) molecular dynamics simulations with AMBER.

(57) Schlegel, B.; Laggner, C.; Meier, R.; Langer, T.; Schnell, D.; Seifert, R.; Stark, H.; Holtje, H. D.; Sippl, W. Generation of a homology model of the human histamine H(3) receptor for ligand docking and pharmacophore-based screening. *J. Comput.-Aided Mol. Des.* **2007**, *21*, 437–453.

(58) Yao, B. B.; Hutchins, C. W.; Carr, T. L.; Cassar, S.; Masters, J. N.; Bennani, Y. L.; Esbenshade, T. A.; Hancock, A. A. Molecular modeling and pharmacological analysis of species-related histamine H(3) receptor heterogeneity. *Neuropharmacology* **2003**, *44*, 773–786.